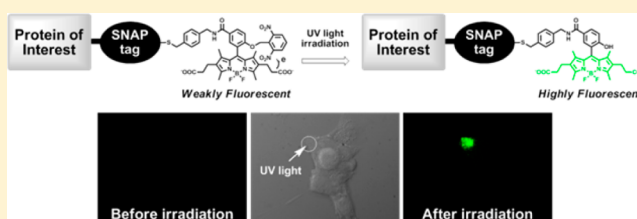


Highly Activatable and Environment-Insensitive Optical Highlighters for Selective Spatiotemporal Imaging of Target Proteins

Tomonori Kobayashi,^{†,||} Toru Komatsu,[†] Mako Kamiya,[‡] Cláudia Campos,^{§,⊥} Marcos González-Gaitán,[§] Takuya Terai,[†] Kenjiro Hanaoka,[†] Tetsuo Nagano,[†] and Yasuteru Urano^{*,†,‡,∇}[†]Graduate School of Pharmaceutical Sciences and [‡]Graduate School of Medicine, The University of Tokyo, 7-3-1 Hongo, Bunkyo-ku, Tokyo 113-0033, Japan[§]Departments of Biochemistry and Molecular Biology, Faculty of Sciences, Geneva University, 30 Quai Ernest-Ansermet, 1211 Geneva, Switzerland

S Supporting Information

ABSTRACT: Optical highlighters are photoactivatable fluorescent molecules that exhibit pronounced changes in their spectral properties in response to irradiation with light of a specific wavelength and intensity. Here, we present a novel design strategy for a new class of caged BODIPY (4,4-difluoro-4-bora-3a,4a-diaza-s-indacene) fluorophores, based on the use of photoremovable protecting groups (PRPGs) with high reduction potentials that serve as both a photosensitive unit and a fluorescence quencher via photoinduced electron transfer (PeT). 2,6-Dinitrobenzyl (DNB)-caged BODIPY was efficiently photoactivated, with activation ratios exceeding 600-fold in aqueous solutions. We then combined this photoactivatable fluorophore with a SNAP (mutant of O⁶-alkylguanine DNA alkyltransferase) ligand to obtain a small-molecule-based optical highlighter for visualization of protein dynamics, using the well-established SNAP tag technology. As proof of concept, we demonstrate spatiotemporal imaging of the fusion protein of epidermal growth factor receptor (EGFR) with SNAP tag in living cells. We also demonstrate highlighting of cells of interest in live zebrafish embryos, using the fusion protein of histone 2A with SNAP tag.



■ INTRODUCTION

Optical highlighters¹ have been developed for visualizing, tracking, and quantifying molecular events in living cells with high spatial and temporal resolution. They are generally photoactivatable fluorescent proteins (PAFPs),² which exhibit pronounced changes in their spectral properties in response to irradiation with light of a specific wavelength and intensity. Although these genetically encoded tags are undoubtedly powerful general tools for imaging proteins within living systems,^{3,4} they are not without limitations. For example, these relatively large molecules can significantly perturb the structure of proteins to which they are attached. Further, most of them lose their fluorescence under acidic conditions, so that they are not applicable to imaging of endocytotic processes, for example. In recent years, an alternative strategy for specifically tagging proteins has emerged that blends the simplicity of genetically encoded tags with the versatility of small-molecular probes.⁵ This approach involves the incorporation of a unique chemical functionality or mutated enzyme into the target protein. These reporters are small, noninvasive, and nonperturbing handles that can be modified in living systems through highly selective reactions with exogenously delivered probes. In this strategy, photoactivatable (caged) fluorophores⁶ are required. In general, caged fluorophores are weakly fluorescent or nonfluorescent when essential functional groups for fluorescence emission are masked by photoremovable protecting groups (PRPGs). Photo-

activation with ultraviolet (UV) light removes the PRPG (uncaging) and abruptly switches on the fluorescence of the parent fluorophore. The requirements for an effective caged fluorophore are rapid and efficient photoactivation, good brightness, and photostability of the uncaged fluorophore. We have already developed a rapidly releasable and highly activatable caged fluorophore based on a novel fluorescein derivative (caged TokyoGreen).⁷ However, the xanthene fluorophore used in TokyoGreen is pH-sensitive, like fluorescent proteins. BODIPY (4,4-difluoro-4-bora-3a,4a-diaza-s-indacene)^{8,9} is a widely used fluorescent dye, which has many features that make it suitable for bioimaging, including high fluorescence quantum efficiency (Φ_f), photostability, excitation at the visible light wavelength (>500 nm), high molecular extinction coefficient, and pH or environmental insensitivity of fluorescence. However, caged BODIPY has never been developed because BODIPY has no functional group for direct fluorescence regulation, unlike other fluorophores. However, we developed a novel molecular design based on intramolecular photoinduced electron transfer (PeT).¹⁰ We have shown that fluorophores bearing electron-deficient moieties are almost nonfluorescent because singlet excited state energy is lost as a consequence of PeT.¹¹ *ortho*-Nitrobenzyl groups are the most representative PRPGs, and are

Received: December 28, 2011

Published: June 13, 2012

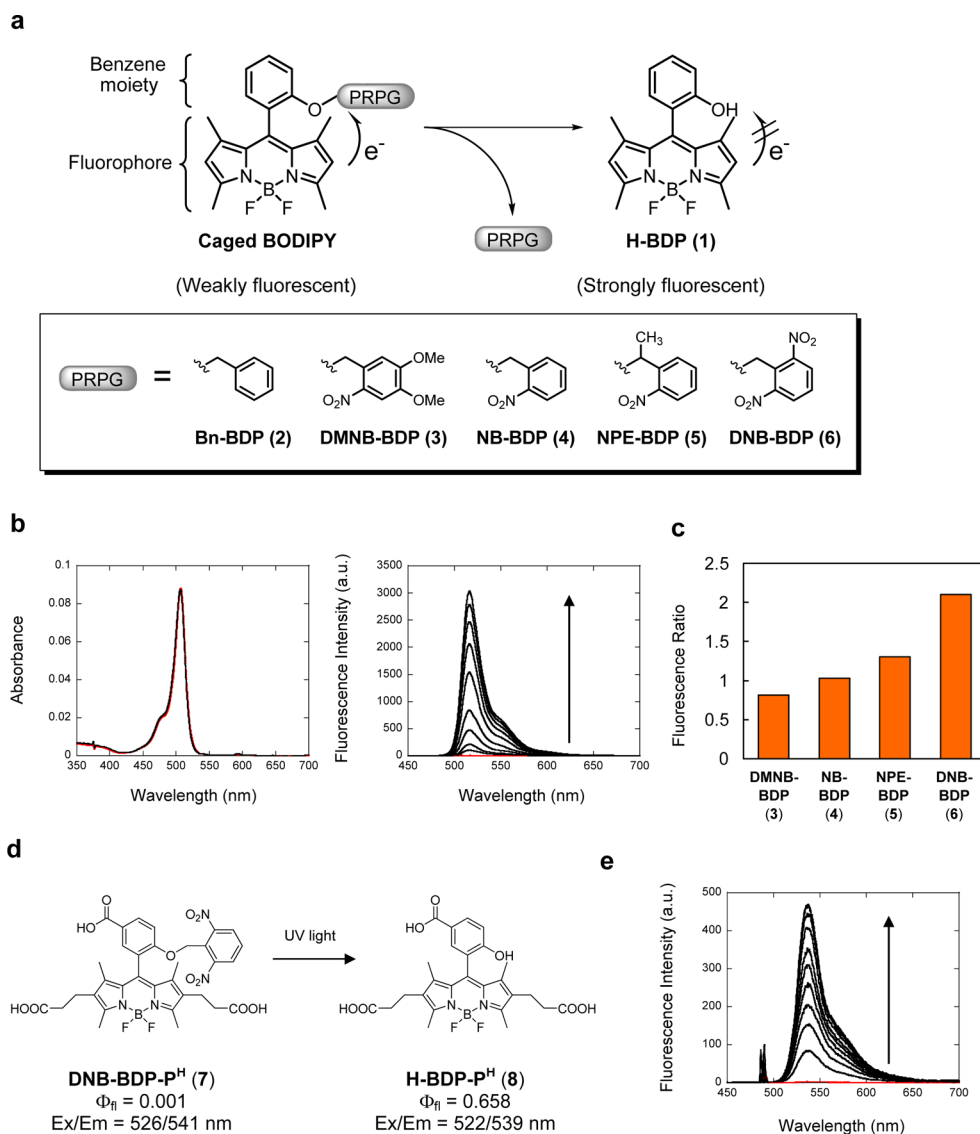


Figure 1. Spectral properties of caged BODIPY. (a) Molecular design of *ortho*-nitrobenzyl caged BODIPY. (b) Absorption (left) and fluorescence (right) spectral change of DNB-BDP (6, 1 μ M) in chloroform upon UV irradiation at around 350 nm (1.25 mW/cm² at 350 nm). Absorption spectra were recorded before (red line) and after irradiation (60 min). Fluorescence spectra were recorded after the specified duration of UV irradiation; 0 (red line), 1, 2, 5, 10, 20, 30, 40, 50, 60 min (black line). (c) Fluorescence ratio values at the emission maximum wavelength upon UV irradiation in chloroform. Fluorescence ratio denotes the ratio of the fluorescence intensity after 120 s UV irradiation with respect to the fluorescence intensity before irradiation at the emission maximum wavelength. (d) Photoactivation diagram of water-soluble DNB-caged BODIPY (DNB-BDP-P^H, 7). (e) Fluorescence spectral change of DNB-BDP-P^H (1 μ M) in sodium phosphate buffer (pH 7.4) upon UV irradiation at around 350 nm (1.25 mW/cm² at 350 nm). Fluorescence spectra were recorded after the specified duration of UV irradiation; 0 (red line), 10, 20, 30, 40, 50, 60, 80, 100, 120, and 150 min (black line).

also strongly electron-deficient.¹² So, we expected that conjugation of *ortho*-nitrobenzyl groups to a BODIPY fluorophore would result in fluorescence quenching via a PeT process, while photodeprotection would result in loss of PeT, with recovery of the fluorescence. Here, we report rational design of caged BODIPY and its application to optical highlighting of epidermal growth factor receptor (EGFR) in living cells and cells of interest in live zebrafish embryo by utilizing the well-established SNAP (a mutant of *O*⁶-alkylguanine-DNA alkyl-transferase) tag technology.

RESULTS

Molecular Design of Caged BODIPY. The structures of caged BODIPY are shown in Figure 1a. We chose the 8-phenyl-

1,3,5,7-tetramethyl BODIPY skeleton as a platform for the following two reasons: (1) it has a high value of Φ_f due to its sterically constrained structure,¹³ and (2) many varieties of functional groups can be introduced into the 8-phenyl group for fluorescence regulation or bioconjugation. The structure can be considered as consisting of two orthogonal parts, the benzene moiety and the fluorophore, since they are twisted and conjugatively uncoupled. As PRPGs, we chose four *ortho*-nitrobenzyl derivatives with different electrochemical and photochemical properties, that is, 4,5-dimethoxy-2-nitrobenzyl (DMNB), 2-nitrobenzyl (NB), 1-(2-nitrophenyl)ethyl (NPE), and 2,6-dinitrobenzyl (DNB) groups. A benzyl (Bn)-protected derivative was designed as a control compound. *ortho*-Nitrobenzyl groups can protect a variety of functional groups. Among them, we chose a phenolic group as a caging site, because the

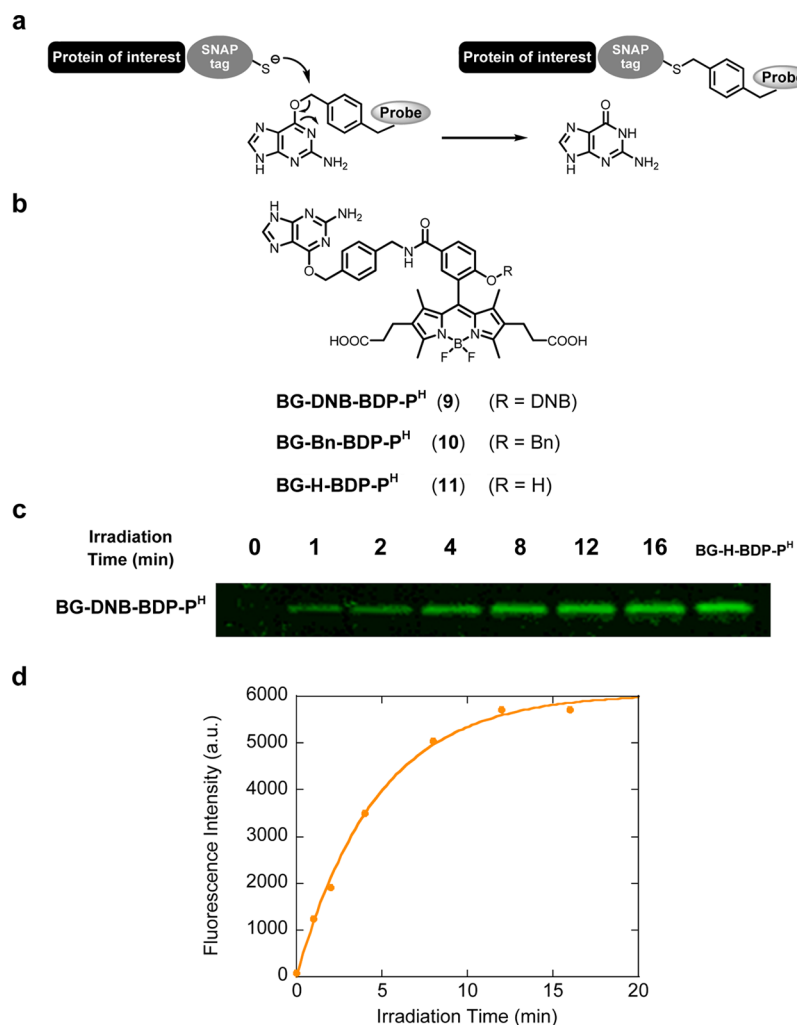


Figure 2. Photoactivation experiments with the DNB-BDP-P^H-SNAP complex *in vitro*. (a) Covalent labeling of a SNAP-fusion protein using O⁶-benzylguanine (BG) derivatives. (b) Structures of caged BODIPY-SNAP ligands. (c) Fluorescence image of an SDS-PAGE gel after irradiation. SNAP (0.5 μ M) was incubated for 2.5 h in the presence of BG-DNB-BDP-P^H (9, 10 μ M). After completion of labeling, the solutions were irradiated with UV light (365 nm) for various periods of time (0, 1, 2, 4, 8, 12, 16 min). The irradiated solution was denatured by heating, and then subjected to SDS-PAGE. (d) Fluorescence intensity of the SNAP band.

ether bond is stable under physiological conditions. Another important point is the substitution position in the benzene moiety. Generally, PeT is less effective with increasing distance between the fluorophore and the quencher.¹⁴ Therefore, it should be preferable to conjugate PRPGs at the nearest position to the fluorophore. It should also be noted that there is only a single *ortho*-nitrobenzyl group, and so the caged BODIPY is expected to be rapidly activated, compared to traditional bis-caged fluorescein or rhodamine.⁷ Also, the photogenerated byproduct (*ortho*-nitrosobenzaldehyde) is expected to show low cytotoxicity.

Synthesis and Spectroscopic Properties of Caged BODIPY and Relationship between Fluorescence Quantum Yield and Reduction Potential of the Electron Acceptor. As shown in Supporting Information Figure S1, 2-hydroxybenzaldehyde, used as a starting material, was protected with a benzyl group, followed by condensation with 2,4-dimethylpyrrole in the presence of trifluoroacetic acid, oxidation with 2,3-dichloro-5,6-dicyano-*p*-benzoquinone, and coordination of boron trifluoride diethyl etherate to give Bn-BDP (2). The benzyl group was removed by catalytic reduction to afford the photoproduct, H-BDP (1). Three caged derivatives, DMNB-

BDP (3), NB-BDP (4), and NPE-BDP (5), were synthesized from the corresponding benzaldehydes in the same manner as described for Bn-BDP. With regard to the dinitrobenzyl derivative (DNB-BDP, 6), the corresponding benzaldehyde could not be obtained because of the formation of byproduct. Therefore, we used the corresponding acetal to obtain DNB-BDP. The Φ_{fl} values of caged BODIPY in various organic solvents are summarized in Supporting Information Table S1. Their absorption spectra were almost the same in every solvent, except that DMNB-BDP had higher absorbance in the 350–400 nm region (Supporting Information Figure S2). The photoproduct H-BDP was highly fluorescent in every solvent. Bn-BDP, the control compound with no nitro group, was as highly fluorescent as H-BDP. In contrast, all nitrobenzyl-caged BODIPYs were less fluorescent than Bn-BDP, although the Φ_{fl} values differed to some extent from compound to compound. The value of Φ_{fl} was the smallest for DNB-BDP, followed by NPE-BDP, NB-BDP, and DMNB-BDP. The corresponding benzene moiety of each caged BODIPY was independently synthesized and their reduction potentials were examined by means of cyclic voltammetry. Their reduction potentials in acetonitrile were in the order DNB > NPE > NB > DMNB > Bn,

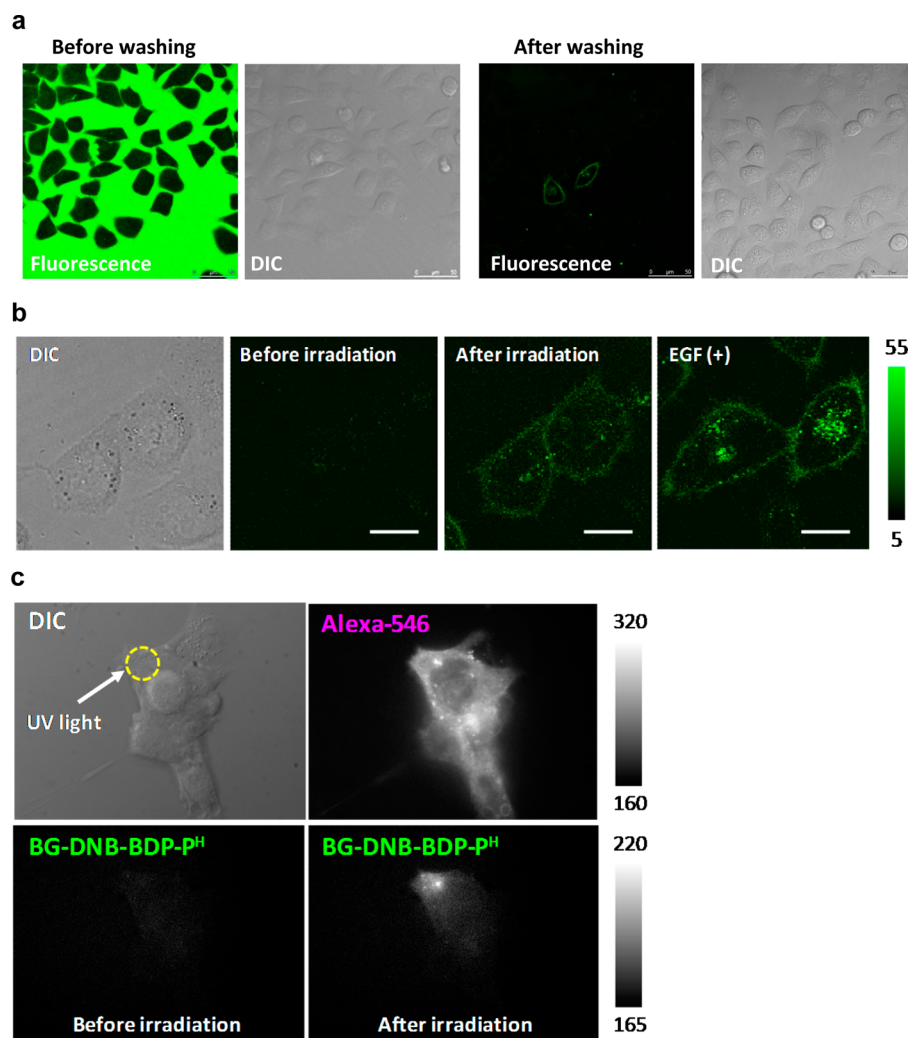


Figure 3. Optical highlighting of EGFR-SNAP fusion protein. (a) Confocal fluorescence image of BG-Bn-BDP-PH (**10**, 2 μ M)-loaded HeLa cells transiently expressing EGFR-SNAP protein before washing (left panel) and after washing (right panel). (b) Confocal fluorescence image of BG-DNB-BDP-PH (**9**, 2 μ M)-loaded HeLa cells transiently expressing EGFR-SNAP protein before and after UV irradiation. UV irradiation was carried out at the whole field for 5 min by a handy-held UV lamp (365 nm, 1.5 mW/cm²). After EGF addition to the irradiated cell culture (final concentration: 100 ng/mL) and incubation at 37 °C for 3 h, a fluorescence image was captured. Scale bar: 15 μ m. (c) Epifluorescence images of BG-DNB-BDP-PH (**2** μ M)-loaded COS-7 cells transiently expressing EGFR-SNAP protein before and after UV irradiation. Localized UV irradiation was carried out for 30 s through an objective lens with a pinhole. EGFR-SNAP expressing cells were marked with a cell-impermeable fluorescent marker, BG-Alexa-546 (2 μ M), after labeling with BG-DNB-BDP-PH (2 μ M).

in agreement with the values of Φ_{fl} . To provide further evidence for fluorescence regulation based on PeT, we prepared methoxy- and fluorine-substituted caged BODIPYs. It was reported that the oxidation potential of methoxy-substituted BODIPY was greatly decreased compared to those of fluorine-substituted derivatives without any change in the spectral properties.¹⁵ For almost all the caged derivatives, the Φ_{fl} was decreased for methoxy derivatives compared to fluorine derivatives (Supporting Information Table S1).

Photoactivation Experiments in Cuvette. Solutions of caged BODIPY were illuminated with UV light from a 500 W xenon lamp equipped with a monochromator system, with stirring. Experiments were initially carried out in five organic solvents (acetonitrile, methanol, acetone, dichloromethane, and chloroform). Representative changes of the absorbance and fluorescence spectra of DNB-BDP upon UV irradiation in chloroform are shown in Figure 1b. H-BDP was generated, with a concomitant fluorescence increase, upon irradiation of DNB-BDP, as confirmed by comparison of the ¹H NMR spectra with

that of an authentic sample (Supporting Information Figure S3). Fluorescence ratio values upon illumination in chloroform are shown in Figure 1c. Among the compounds, DNB-BDP showed the largest fluorescence ratio value. Similar results were obtained in other solvents (Supporting Information Figure S4). Next, we synthesized a water-soluble DNB-caged BODIPY in order to examine photoactivatability in aqueous solution. To improve the water solubility, we introduced a carboxylic acid into the benzene moiety and two propionates into the fluorophore (DNB-BDP-PH, **7**, Figure 1d). The fluorescence of DNB-BDP-PH was strongly quenched (Φ_{fl} = 0.001) in pH 7.4 buffered aqueous solution, and a dramatic fluorescence increase (>600-fold) was observed upon generation of the photoproduct (H-BDP-PH, **8**, Φ_{fl} = 0.658) by means of UV irradiation (Figure 1e). The uncaging cross section (product of molar extinction coefficient and uncaging quantum yield) of DNB-caged BODIPY was 50 M⁻¹ cm⁻¹ ($\epsilon_{350 \text{ nm}}$ = 5.6×10^3 M⁻¹ cm⁻¹, Φ_{uncage} = 8.9×10^{-3}), which is comparable to those of other *ortho*-nitrobenzyl caged compounds (Supporting Information Figure S5).¹⁶ Rhodamine

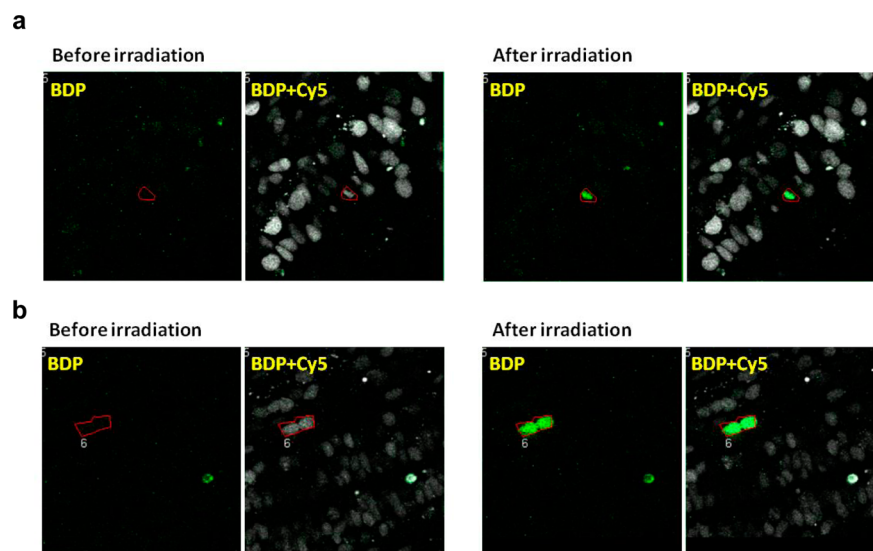


Figure 4. Optical highlighting of cells of interest in a zebrafish embryo. (a and b) Confocal fluorescence images of embryonic spinal cord. The embryos were injected with H2A-SNAP and double-stained with BG-DNB-BDP- P^H and BG-Cy5. Before irradiation, one (a) or two (b) nuclei were selected based on Cy5 fluorescence (regions surround by red line), and were clearly highlighted upon irradiation with a 405 nm laser.

is another candidate for a photobleaching-resistant fluorophore. We have applied this strategy to rhodamine, and synthesized NPE-caged and DNB-caged tetramethylrhodamine (TMR) (Supporting Information Figure S6a). We found that the fluorescence of these compounds was efficiently quenched in aqueous solution, but serious photobleaching occurred with UV illumination, as can be seen in the absorption spectra (Supporting Information Figure S6b and S6c). The photoproduct 2-OH TMR did not show much photobleaching (Supporting Information Figure S6d), so an unexpected reaction involving the *ortho*-nitrobenzyl moiety might have occurred in these cases.

Environment-Insensitivity of Caged BODIPY. We examined the environment-insensitivity of the fluorescence of DNB-caged BODIPY. Fluorescence of DNB-caged BODIPY was efficiently quenched ($\Phi_q < 0.01$) in various solvents from polar to nonpolar solvents (Supporting Information Table S1). Although another PeT-regulated dye, DNB-caged TokyoGreen, has low initial fluorescence under aqueous conditions, it emits moderate fluorescence without photoactivation in less polar environments, such as methanol or at a protein surface (Supporting Information Figures S7 and S8). DNB-caged BODIPY was stable at physiological pH and in the presence of some reducing enzymes (Supporting Information Figures S9 and S10). Additionally, we synthesized the photoproduct and examined its pH sensitivity. It emitted stable fluorescence in acidic solutions from pH 2 to 7 (Supporting Information Figure S11).

Synthesis of Caged BODIPY-SNAP Ligand and Its Reaction Rate with SNAP and Photoactivatability. To examine the feasibility of using our fluorophores for small-molecule-based optical highlighting, we used the SNAP tag technology to specifically label target proteins.¹⁷ SNAP protein is derived from *O*⁶-alkylguanine-DNA alkyltransferase (AGT), which reacts covalently with benzylguanine (BG). This tag can be specifically and covalently labeled with any fluorophore carried by the benzyl group of BG (Figure 2a). Thus, we designed and synthesized caged BODIPY-SNAP ligand (BG-DNB-BDP- P^H , **9**), a fluorescent analogue (BG-Bn-BDP- P^H , **10**), and the photoproduct (BG-H-BDP- P^H , **11**) (Figure 2b). They were designed to be hydrophilic and membrane-impermeable so that

they could be easily washed out. BG was appended onto the benzene moiety via an amide bond, and two propionates were introduced into the fluorophore to increase the water solubility. The reaction kinetics of these substrates with purified SNAP-GST *in vitro* were comparable with that of a standard fluorogenic substrate, BGFL (Supporting Information Figure S12). Non-specific binding was not observed when BG-Bn-BDP- P^H was incubated with SNAP-GST in the presence of bovine serum albumin (Supporting Information Figure S13). Next, we examined the photoactivatability of DNB-BDP- P^H -SNAP complex *in vitro*. After completion of labeling in aqueous solution buffered at pH 7.4, DNB-BDP- P^H -SNAP complex was UV-irradiated for various periods of time. The fluorescence intensity of the SNAP band increased in an irradiation time-dependent manner (Figure 2c,d).

Optical Highlighting of EGFR-SNAP Fusion Protein with Caged BODIPY-SNAP Ligand. We selected epidermal growth factor receptor (EGFR) as a target to test the validity of our approach, since sufficient structural information is available to design a fusion protein.^{18,19} We prepared a gene construct for a fusion protein of EGFR with SNAP. After transient transfection using standard liposome-mediated gene transfer techniques, HeLa cells were incubated with BG-Bn-BDP- P^H , a fluorescent analogue, in order to identify optimal labeling conditions under a fluorescence microscope. BG-Bn-BDP- P^H was membrane-impermeable, and nonspecific binding or accumulation of free dye was not observed (Figure 3a). Then, we attempted optical highlighting of EGFR-SNAP with BG-DNB-BDP- P^H . After labeling and washout of the unreacted probes, cells in the whole field were irradiated with a handy UV lamp (365 nm). Fluorescence increase was observed in transfected cells, and following EGF stimulation resulted in internalization of EGFR (Figure 3b). Further, we demonstrated localized photoactivation experiments using pulse-chase labeling techniques (Figure 3c). First, COS-7 cells transiently expressing EGFR-SNAP protein were incubated with BG-DNB-BDP- P^H and unreacted dye was washed out. Then, the cells were pulse-labeled with a red-fluorescent substrate, BG-Alexa-546 (top panel, right). UV light was focused to the small area of the cells showing red fluorescence and irradiated through an objective lens under an

epifluorescence microscope. After irradiation, we observed an increase of fluorescence intensity at the irradiated site (bottom panel), with subsequent fluorescence decay due to lateral diffusion and vesicular trafficking of EGFR-SNAP (Supporting Information Figure S14 and Movie 1).^{20,21}

We also checked the pH-insensitivity of BODIPY dyes in living cells. HeLa cells expressing EGFR-SNAP were labeled with BG-H-BDP-P^H, the photoproduct of our caged substrates, and with BGFL, a BG derivative of caged fluorescein. The fluorescence of BGFL is known to be quenched under slightly acidic conditions owing to the formation of a protonated form, that is, it is pH-sensitive. Before EGF stimulation, EGFR in plasma membrane was labeled in the same way with each of the probes (Supporting Information Figure S15a). After EGF stimulation, a part of EGFR was internalized through endocytosis and could be observed as fluorescent vesicles. Next, we added ammonium chloride to neutralize these acidic vesicles (Supporting Information Figure S15b). The fluorescence intensity did not change significantly in the BODIPY-labeled cells, whereas that of the BGFL-labeled cells increased by ~40%. After washout of ammonium chloride, the fluorescence intensity reverted to the original value.

Optical Highlighting of Target Nuclei in Zebrafish Embryo with Caged BODIPY-SNAP Ligand. As another application of our probe, we tried *in vivo* optical highlighting of target nuclei in zebrafish embryo. We have previously demonstrated that the combination of SNAP-tag with photoactivatable substrates can be used for this purpose.²² To investigate whether our newly developed BG-DNB-BDP-P^H can also be applied for highlighting cells of interest in living zebrafish embryo, we injected embryos at the one-cell stage with H2A-SNAP RNA and BG-DNB-BDP-P^H/BG-Cy5. The embryos were allowed to develop for 24 h, then a selected single nucleus (Figure 4a, Supporting Information Movie 2) or two nuclei (Figure 4b, Supporting Information Movie 3) were illuminated with 405 nm laser light. We observed a marked fluorescence increase only in the illuminated nuclei, confirming that our probe can be used for highlighting cells of interest in the developing embryo.

DISCUSSION

Here, we have proposed a novel concept for molecular design of caged fluorophores, as exemplified by caged BODIPYs. The basis of this approach is that PRPGs with high reduction potentials can be used as both a fluorescence quencher via a PeT process and a photosensitive unit (Figure 1a). In general, the feasibility of electron transfer between a fluorophore and a quencher can be judged from the change in Gibbs free energy (ΔG_{eT}). The ΔG_{eT} value can be calculated from measurable parameters by use of the Rehm–Weller equation,²³ as follows:

$$\Delta G_{\text{eT}} = E_{\text{ox}} - E_{\text{red}} - E_{00} - C$$

where E_{ox} and E_{red} are the oxidation potential of the electron donor and the reduction potential of the electron acceptor, respectively, E_{00} is the singlet excited energy of the fluorophore, and C is the work term for the charge separation state. In the case of caged BODIPY, all compounds have the same absorption maxima, so that the E_{00} values can be determined easily. The values of C may also be similar in view of the structural similarity of the compounds. As a result, the efficiency of PeT can be compared just in terms of E_{ox} and E_{red} of the fluorophore and benzene moieties, respectively. The Φ_{fl} of caged BODIPY correlated well with E_{red} of the corresponding benzene moieties in the same fluorophore or E_{ox} of the fluorophores in the same

PRPGs (Supporting Information Table S1). The above results suggest that our PeT-regulated photoswitching design strategy has worked efficiently.

Photoactivation experiments in cuvette showed that DNB-caged BODIPY had the best properties as a caged fluorophore (Figure 1b–e). DNB-BDP had the highest fluorescence activation ratio among the four derivatives. NPE-BDP gave a comparable fluorescence increase, but the fluorescence ratio value was smaller because of its moderate initial fluorescence (Supporting Information Figure S4). It was essential to use the 2,6-dinitrobenzyl group in our case from the viewpoint of obtaining efficient PeT to minimize the initial fluorescence. In practical applications, it is very important that the initial fluorescence before photoactivation should be as low as possible in order to obtain high-contrast fluorescence images. Here, we should emphasize the point that in the design of caged fluorophores based on the PeT mechanism, not only the photochemical properties (such as Φ_{uncage} , molar extinction coefficient, and reaction rate), but also the electrochemical properties of PRPGs are critically important to achieve high photoactivation fluorescence efficiency; this is different from the case of usual caged bioactive compounds.

The DNB-caged BODIPY described here has several advantages over traditional caged fluorophores. First, the initial fluorescence of DNB-caged BODIPY is very low in solvents with different polarity from water to chloroform, unlike that of another PeT-regulated caged fluorophore, caged TokyoGreen (Supporting Information Figures S7 and S8).⁷ Second, uncaged BODIPY emits stable fluorescence insensitive to changes of solvent polarity (Supporting Information Table S1) or pH (Supporting Information Figure S11). In contrast, fluorescein²⁴ or coumarin²⁵ dyes have acidic groups in the fluorophore, and their emissions are influenced by pH change around the physiological range. Third, it can be activated by single-step deprotection of PRPG, and therefore, rapid uncaging is possible with minimal UV irradiation, whereas bis-caged fluorescein or rhodamine require more prolonged illumination.

As a practical application to demonstrate the utility of our approach, we investigated optical highlighting of EGFR. Small-molecule-based optical highlighting has faced the critical problem that selective labeling techniques for target molecules *in situ* were not available, and consequently, nonspecific labeling and dye accumulation within cells generated nontarget-derived signals, so that quantitative analysis was impossible. Recently, however, some promising techniques have emerged such as SNAP tag,¹⁷ Halotag,²⁶ and tetracycline tag²⁷ for protein labeling *in situ*. Among them, SNAP tag technology is commercially available and has been used for many biological studies (Figure 2a). So, we designed a caged BODIPY-SNAP ligand and its derivatives with suitable labeling kinetics for biological application (Figure 2b). Caged BODIPY-SNAP complex worked efficiently *in vitro* (Figure 2c,d), and so we next tried optical highlighting in living cells. After UV irradiation of the whole field (Figure 3b) or a localized site (Figure 3c), fluorescence increase was observed in transiently EGFR-SNAP-expressing cells. Further, pH-insensitivity of BODIPY probes was confirmed by the lack of fluorescence change in response to neutralization of acidic vesicles containing the fusion protein (Supporting Information Figure S15). These experiments successfully demonstrated the optical highlighting of a target protein in living cells. As another application of our probes, we demonstrated optical highlighting of zebrafish nuclei (Figure 4a,b). After injection of BG-DNB-BDP-P^H and 405 nm laser

illumination, a marked fluorescence increase was observed only in the illuminated nuclei. This result suggests that caged BODIPY could be a useful tool for cell lineage analysis in developmental biology.

In this case, the SNAP tag is nearly as large as fluorescent proteins. However, there are smaller and less perturbing tag systems, such as tetracycline²⁷ or BODIPY/diacrylate tags,²⁸ and their use should make it possible to optically highlight a target protein with relatively little influence on its function. Moreover, small-molecule-based optical highlighting techniques should be applicable to biomolecules other than proteins, such as glycans or lipids. Recently, bioorthogonal chemical reporter selective labeling technologies,⁵ such as copper-free click chemistry²⁹ or Staudinger ligation,³⁰ have been developed and applied to many biological studies. It should be possible to introduce these reactive moieties into caged BODIPYs using simple methods of organic synthesis. Another important application of caged fluorophores is superresolution microscopy, such as PALM (photoactivation localized microscopy).³¹ Recently, Banala reported the application of a caged rhodamine110 derivative/SNAP tag for superresolution microscopy, obtaining a high photon yield compared to that in the case of fluorescent proteins.³² Likewise, our caged BODIPY/SNAP tag is also expected to contribute to the color pallet of small-molecule-based optical highlighters.

CONCLUSION

We have developed small-molecule-based optical highlighters with high activation ratio and environmental insensitivity (polarity or pH), by combining a new class of caged BODIPY fluorophores with SNAP tag technology. We confirmed the usefulness of this approach for two applications: optical highlighting of (1) EGFR in cells expressing EGFR-SNAP fusion protein, and (2) selected cells in zebrafish embryo expressing H2A-SNAP fusion protein. We are currently working to extend this approach for optical highlighting of small biomolecules other than proteins.

ASSOCIATED CONTENT

Supporting Information

Experimental conditions; supplementary methods for chemical synthesis and characterization of compounds; supplementary experiments and data; Figures S1–S15; Table S1; supplementary movies 1–3; complete ref 26. This material is available free of charge via the Internet at <http://pubs.acs.org>.

AUTHOR INFORMATION

Corresponding Author

*To whom correspondence should be addressed. E-mail: uranokun@m.u-tokyo.ac.jp

Present Addresses

^{||}Chemistry Research Laboratories, Dainippon Sumitomo Pharma Co. Ltd., 33-94 Enoki-cho, Suita Osaka 564-0053, Japan

[⊥]Instituto Gulbenkian de Ciência, R. da Quinta Grande n°6, 2780-156 Oeiras, Portugal

[▽]Basic Research Program, Japan Science and Technology Agency, 7 Gobancho, Chiyoda-ku, Tokyo 102-0076, Japan.

Notes

The authors declare no competing financial interest.

ACKNOWLEDGMENTS

We thank Dr. Haruhiko Bito, Dr. Hiroyuki Okuno, and Yayoi Kondo in the University of Tokyo for their technical support in DNA and cellular experiments. This work was financially supported by the Ministry of Education, Culture, Sports, Science and Technology of Japan (Grants for The Advanced and Innovative Research Program in Life Sciences, 16370071 and 16659003, Grants 20117003 and 23249004 to Y.U., and 23113504 to M.K.). T.N. was also supported by the Hohansha Foundation. C.C. was supported by FCT (SFRH/BD/15210/2004), Oncasym and Programa Gulbenkian de Doutoramento em Biomedicina. M.G.-G. and C.C. were supported by the Swiss National Science Foundation, grants from the Swiss SystemsX.ch initiative, and LipidX-2008/011, an ERC advanced investigator grant, NCCR Chemical Biology and the Polish-Swiss research program.

REFERENCES

- (1) Shaner, N. C.; Patterson, G. H.; Davidson, M. W. *J. Cell. Sci.* **2007**, *120*, 4247–4260.
- (2) Berkusha, V. V.; Lukyanov, K. A. *Nat. Biotechnol.* **2004**, *22*, 289–296.
- (3) Patterson, G. H.; Lippincott-Schwartz, J. *Science* **2002**, *297*, 1873–1877.
- (4) Habuchi, S.; Ando, R.; Dedecker, P.; Verheijen, W.; Mizuno, H.; Miyawaki, A.; Hofkens, J. *Proc. Natl. Acad. Sci. U.S.A.* **2005**, *102*, 9511–9516.
- (5) Prescher, J. A.; Bertozzi, C. R. *Nat. Chem. Biol.* **2005**, *1*, 13–21.
- (6) Puliti, D.; Warther, D.; Orange, C.; Specht, A.; Goeldner, M. *Bioorg. Med. Chem.* **2011**, *19*, 1023–1029.
- (7) Kobayashi, T.; Urano, Y.; Kamiya, M.; Ueno, T.; Kojima, H.; Nagano, T. *J. Am. Chem. Soc.* **2007**, *129*, 6696–6697.
- (8) Ulrich, G.; Ziessel, R.; Harriman, A. *Angew. Chem., Int. Ed.* **2008**, *47*, 1184–1201.
- (9) Loudet, A.; Burgess, K. *Chem. Rev.* **2007**, *107*, 4891–4932.
- (10) De Silva, A. P.; Gunaratne, H. Q. N.; Gunnlaugsson, T.; Huxley, A. J. M.; McCoy, C. P.; Rademacher, J. T.; Rice, T. E. *Chem. Rev.* **1997**, *97*, 1515–1566.
- (11) Ueno, T.; Urano, Y.; Setsukinai, K.; Takakusa, H.; Kojima, H.; Kikuchi, K.; Ohkubo, K.; Fukuzumi, S.; Nagano, T. *J. Am. Chem. Soc.* **2004**, *126*, 14079–14085.
- (12) Pillai, V. N. R. *Synthesis* **1980**, *1*, 1–26.
- (13) Cui, A.; Peng, X.; Fan, J.; Chen, X.; Wu, Y.; Guo, B. *J. Photochem. Photobiol., A* **2007**, *186*, 85–92.
- (14) Matsumoto, T.; Urano, Y.; Shoda, T.; Kojima, H.; Nagano, T. *Org. Lett.* **2007**, *9*, 3375–3377.
- (15) Gabe, Y.; Ueno, T.; Urano, Y.; Kojima, H.; Nagano, T. *Anal. Bioanal. Chem.* **2006**, *386*, 621–626.
- (16) Aujard, I.; Benbrahim, C.; Gouget, M.; Ruel, O.; Baudin, J.; Neveu, P.; Jullien, L. *Chem.—Eur. J.* **2006**, *12*, 6865–6879.
- (17) Keppler, A.; Gendrezig, S.; Gronemeyer, T.; Pick, H.; Vogel, H.; Johnsson, K. *Nat. Biotechnol.* **2003**, *21*, 86–89.
- (18) Carter, R. E.; Sorkin, A. J. *Biol. Chem.* **1998**, *273*, 35000–35007.
- (19) Brock, R.; Hamelers, I. H.; Jovin, T. M. *Cytometry* **1999**, *35*, 353–362.
- (20) Lajoie, P.; Partridge, E. A.; Guay, G.; Goetz, J. G.; Pawling, J.; Lagana, A.; Joshi, B.; Dennis, J. W.; Nabi, I. R. *J. Cell Biol.* **2007**, *179*, 341–356.
- (21) Sorkin, A.; von Zastrow, M. *Nat. Rev. Mol. Cell Biol.* **2002**, *3*, 600–614.
- (22) Campos, C.; Kamiya, M.; Banala, S.; Johnsson, K.; González-Gaitán, M. *Dev. Dyn.* **2011**, *240*, 820–827.
- (23) Rehm, D.; Weller, A. *Isr. J. Chem.* **1970**, *8*, 259–271.
- (24) Zheng, G.; Guo, Y. M.; Li, W. *J. Am. Chem. Soc.* **2007**, *129*, 10616–10617.
- (25) Zhao, Y.; Zheng, Q.; Dakin, K.; Xu, K.; Martinez, M. L.; Li, W. *J. Am. Chem. Soc.* **2004**, *126*, 4653–4663.

- (26) Los, G. V.; et al. *ACS Chem. Biol.* **2008**, 3, 373–382.
- (27) Griffin, B. A.; Adams, S. R.; Tsien, R. Y. *Science* **1998**, 281, 269–272.
- (28) Lee, J.; Lee, S.; Zhai, D.; Ahn, Y.; Yeo, H.; Tan, Y.; Chang, Y. *Chem. Commun.* **2011**, 47, 4508–4510.
- (29) Laughlin, S. T.; Baskin, J. M.; Amacher, S. L.; Bertozzi, C. R. *Science* **2008**, 320, 664–667.
- (30) Hangauer, M. J.; Bertozzi, C. R. *Angew. Chem., Int. Ed.* **2008**, 47, 2394–2397.
- (31) Betzig, E.; Patterson, G. H.; Sougrat, R.; Lindwasser, O. W.; Olenych, S.; Bonifacino, J. S.; Davidson, M. W.; Lippincott-Schwartz, J.; Hess, H. F. *Science* **2006**, 313, 1642–1645.
- (32) Banala, S.; Maurel, D.; Manley, S.; Johnsson, K. *ACS Chem. Biol.* **2012**, 7, 289–293.